# Time Domain Variable Speed Wind Energy Conversion Systems Modelling Using ATP Platform

F.H.Costa[1], E. B. Alvarenga[1], J. C. Oliveira[1], G. C. Guimarães[1], A. F. Bonelli[2], Z. S. Vitório J[3]

[1] Faculty of Electrical Engineering
UFU, Federal University of Uberlândia
Campus Santa Mônica – Av. João Naves de Ávila, 2121 – Bloco 3N – Uberlândia (Brazil)
Phone/Fax number: +55 34 3239 4733/+55 34 3239 4704, email:**fernandahein@hotmail.com; elias_alvarenga@hotmail.com; jcoliveira@ufu.br; gcaixeta@ufu.br;**
[2] LACTEC – Institute of Technology for Development
Centro politécnico da UFPR – Curitiba, Paraná (Brazil) CEP:81531-980
Phone/fax: +55 41 3361 6868 / +55 41 3361 6007 , e-mail: **arthur.bonelli@lactec.org.br**
[3] Furnas Centrais Elétricas S.A.
Av. Rubens de Mendonça, 2254, 9º andar, Cuiabá-MT (Brazil)
Fone: +55 62 32396529, email: **zelia@furnas.com.br**

**Abstract.** This paper presents a comprehensive computational representation of a variable speed Wind Energy Conversion Systems (WECS) and its connection to typical AC grid systems. The arrangement chosen for modelling purposes consists of a multipole synchronous generators unit. This type of arrangement appears as a modern tendency to WECS composition. The paper content comprises basic information about the overall scheme structure, time domain modelling and computational implementation in the well known ATP platform. Using this approach studies involving transients, dynamic and steady state analysis can be then performed. Although these facilities are available, the case studies here considered are focused on the investigation of the relationship between specific wind and PCC voltage conditions and the final voltage and current forms produced at the AC busbar. Wind energy with distinct ramp and gust conditions are utilized so as to highlight the control action in limiting and optimizing the energy transference to the generators. In addition to this, the occurrence of non-ideal conditions to the PCC voltage and the overall interaction with WECS and AC system can be fully taken into account for power quality studies.

## Key words

Modelling, power quality, variable speed topology, wind energy.

## 1. Introduction

The energy produced by the wind is winning larger prominence because of the great and inexhaustible wind potential available in the world. Having in mind the electrical energy generation possibilities one may consider the use of synchronous and asynchronous generators. Constant speed turbines are usually coupled to induction generators with squirrel cage or wound rotor type. On the other hand, variable speed turbines can be linked to both wound rotor induction generators as well as synchronous generators [1]. The later is the chosen technology here selected to be described, modeled and simulated.

Using the mentioned arrangement, this paper is directed to the description of the physical components of the overall wind generation unit, their modeling using time domain techniques, the implementation in the traditional ATP simulator and, finally, the investigation of the voltage and current waveforms and power quality indexes at the PCC. By performing such studies with a general wind condition and distinct AC voltage supply conditions, relevant information concerning harmonic distortion, voltage unbalance and voltage profile are obtained and compared to the power quality standards requirements.

## 2. Wind Energy Conversion System

The model of the proposed wind turbine is formed by several sub-systems (or representative components), as illustrated in Figure 1.

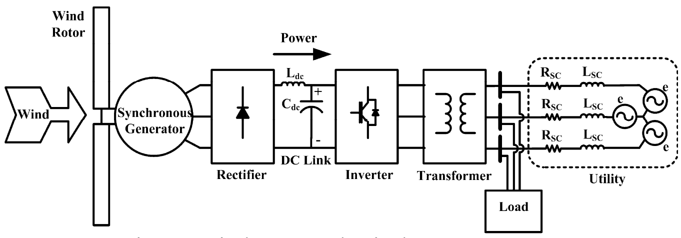


Fig. 1. Wind system physical structure

The mechanical power withdraw from the wind, and supplied to the electric generator shaft, is given by (1) [2] e [3]. In this equation, A represents the area swept by the blades, ρ the specific weight of the air and $V_{wind}$ the wind speed. $C_p$, from (2) to (4), is the power coefficient, corresponding to the Betz limit.

$$P_{mech} = \frac{1}{2}\rho A C_p {V_{wind}}^3 \tag{1}$$

Where:

$$C_p(\lambda,\beta) = 0{,}22\left(\frac{116}{\lambda_i} - 0{,}4\beta - 5\right)e^{\frac{-12{,}5}{\lambda_i}} \tag{2}$$

$$\lambda_i = \frac{1}{\dfrac{1}{\lambda + 0{,}08\beta} - \dfrac{0{,}035}{\beta^3 + 1}} \tag{3}$$

$$\lambda = \frac{V_{blade}}{V_{wind}} = \frac{\omega R}{V_{wind}} \tag{4}$$

And:
β - blade pitch angle;
λ - blade speed ratio (Tip Speed Ratio –TSR).
The speed signal of the incident wind on the rotor blades is represented by the sum of four components, as shown in (5) [4].

$$V_{wind} = V_{base} + V_{gust} + V_{ramp} + V_{noise} \tag{5}$$

Where:
$V_{base}$ - wind base component;
$V_{gust}$ - gust component;
$V_{ramp}$ - ramp component;
$V_{noise}$ - noise component.

The representation of the generator is obtained throughout general flux time domain model of a permanent magnet synchronous machine. The fundamental expressions that relate voltages, fluxes and currents of the synchronous machine are shown in (6) and (7).

$$[V] = -[R_e] * [I] - \frac{d[\lambda_e]}{d_t} \tag{6}$$

$$[\lambda_e] = [L] * [i] \tag{7}$$

Where:
[V], [i], [λe] - column matrices of voltages, currents and linkage fluxes for the stator phases "a", "b" and "c";
[Re] - diagonal resistance matrix of the stator windings "a", "b" and "c";
[L] - inductance matrix of the windings "a", "b", "c" and "F";
The equation to obtain the electromagnetic torque is given by the following expression:

$$T_{elect} = \frac{n_p}{2} F_{IP} \sum_i i_i \frac{dL_{iF}}{d\theta_e} \tag{8}$$

Where:
$n_p$ - number of poles;
$i_i$ - winding currents representing the indexes "a", "b", "c";
$\frac{\mathbf{dL_{iF}}}{\mathbf{d\theta_e}}$ – derivatives of the inductances of the windings of the machine for i assuming: a, b and c;
$F_{IP}$ – magnetic flux from the permanent magnet.

Additionally, the swing equation of a synchronous machine is given by (9).

$$\mathbf{T_T - T_{elect} = J \frac{d_\omega}{d_t}} \tag{9}$$

Where:
$T_T$ - wind turbine torque;
T - electromagnetic torque;
J - inertia moment (wind rotor plus generator rotor).

Out of the several converter topologies available, the choice made in this paper has pointed to the structure shown in Figure 2. It consists of one non-controlled rectifier bridge and a sinusoidal PWM (Pulse Width Modulation) inverter, whose main characteristics are highlighted afterward. In this situation the converter unit behaves like an asynchronous AC-DC-AC link, uncoupling the wind conversion system and the AC electric grid.

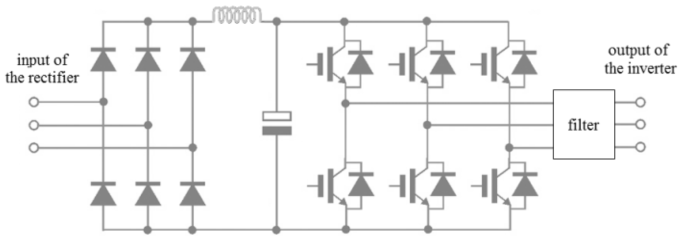


Fig. 2. Frequency converter representation

The inverter makes possible the control of active and reactive powers delivered to/consumed from the system through the proper closed-loop control. The strategy for the control is based on the space vector theory [5] [6] [7] [8] which enables the maximum extraction of the available wind energy.

The low output voltage generated by a wind turbine-system is generally inadequate to attend distribution and transmission requirements. Therefore, there is a need to employ a step-up transformer to connect the WECS to the electric network. This is a conventional ATP transformer model already available in the program library.

The wind system developed is then coupled to an equivalent model of the electric network, formed by an ideal voltage source behind the equivalent impedance (R-L), as shown in Figure 1.

Although a very simple representation has been used, it must be highlighted that the software allows for more comprehensive arrangements so as to cope with real WECS and distribution power quality interaction. However, for this paper purpose the adopted representation was considered appropriate.

The above models were then implemented in the ATP platform throughout the ATPDraw and the Models routines. Due to the lack of space the details are omitted for this paper purposes.

## 3. Case studies and results

The basic data of the turbine employed in the studies are shown in Table I. Using this data, three situations were chosen for this paper investigation purposes. They are:

- *Case 1* – Wind composed of components: base ($V_{base}$= 9m/s), noise, gust ($V_{gust}$= 4.5m/s) and ramp ($V_{ramp}$= 4.5m/s) with the PCC having ideal voltage conditions;

- *Case 2* – The same above conditions with the PCC showing a distorted voltage supply;
- *Case 3* – The same above conditions with the PCC showing an unbalanced voltage supply;

Table I – WECS Data

| | | | | |
|---|---|---|---|---|
| Wind Turbine | n. of blades | Radius [m] | Control | Axis type |
| | 3 | 21 | pitch | horizontal |
| | Speed Rated (m/s) | Cut-in speed (m/s) | Cut-out speed (m/s) | |
| | 12 | 3 | 25 | |
| permanent magnet synchronous machine | Rotor speed (rpm) | p [poles] | $V_r$ [V] | $S_r$ [kVA] |
| | 33.6 | 60 | 600 | 600 |
| Converter | $f_{switching}$ [kHz] | $C_{dc}$ [mF] | $L_{dc}$ [mH] | |
| | 10 | 500 | 1 | |
| | Control | Series reactor at inverter output[mH] | | |
| | space vector | 0.5 | | |
| Transformer | R [%] | Sr [kVA] | $V_1$ [kV] | |
| | 1.0 | 600 | 0.22 | |
| | Z [%] | fr [Hz] | $V_2$ [kV] | |
| | 6.1 | 60 | 13.8 | |
| Utility | $S_{SC}$ [MVA] | Vr [kV] | fr [Hz] | |
| | 20 | 13.8 | 60 | |
| Load | P [kW] | Q [kVAr] | Vr [kV] | fr [Hz] |
| | 500 | 125 | 13.8 | 60 |

*Note: Subscript "r" means "rated" value*

## A. Case 1 results – ideal PCC voltage conditions

Figure 3 shows the wind signal used in this case. The wind profile indicates the presence of the overall wind representation, i.e. a base component, a noise, a gust and a ramp. This characteristic will be used for the other two situations to be later considered.

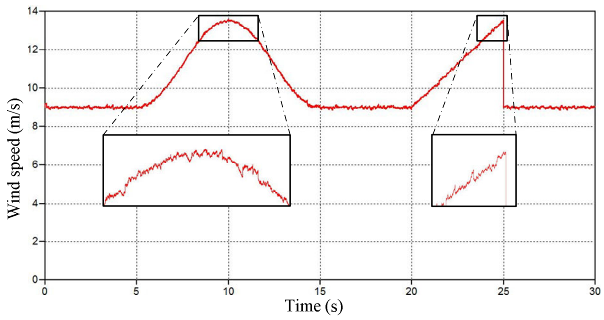


Fig. 3. Wind profile – Case 1.

The corresponding turbine rotor shaft speed is given in Figure 4. This highlights the rotor speed sensitivity to the primary energy source variations. The speed performance makes clear the effect of both the inverter and the Pitch control. The inverter always seeks for an optimum speed to operate with the best Cp, and the pitch control act in such a way as to limit the energy transference to the generator.

Figure 5 provide a typical line voltage zoom for the $v_{ab}(t)$ inverter output at the final wind steady state conditions, i.e, around t=28 s. The three-phase overall voltage profile has been omitted as it does not highlight relevant information other than the amplitude variation along the adopted wind composition. Besides, the figure would be quite confusing at identifying the other voltage waveforms as they are very similar.

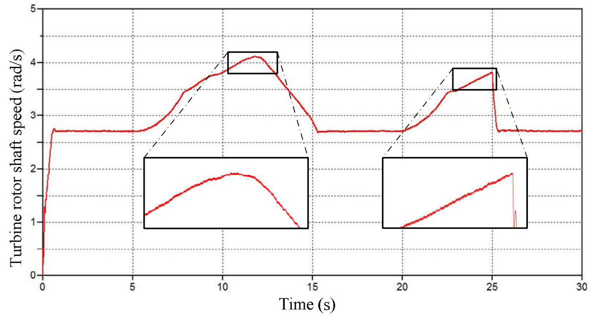


Fig. 4. Wind turbine shaft speed – Case 1

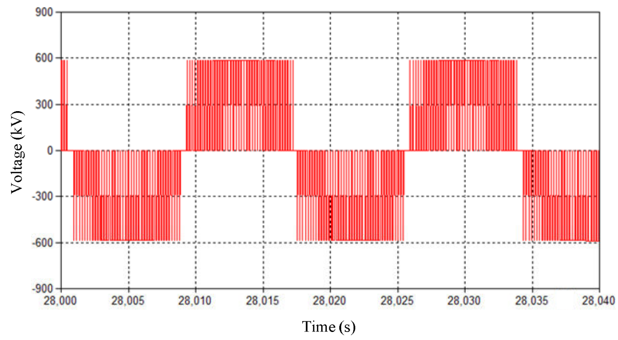


Fig. 5. Line voltage zoom waveform at inverter output with steady state 9m/s wind conditions – $v_{ab}$ - Case 1

In a complementary way, Figure 6 shows the three-phase line voltage zooms at the PCC. It can be seen that the voltage waveforms are practically sinusoidal. The values have remained at approximately 13.72 kV and the THD was found to be less than 1%.

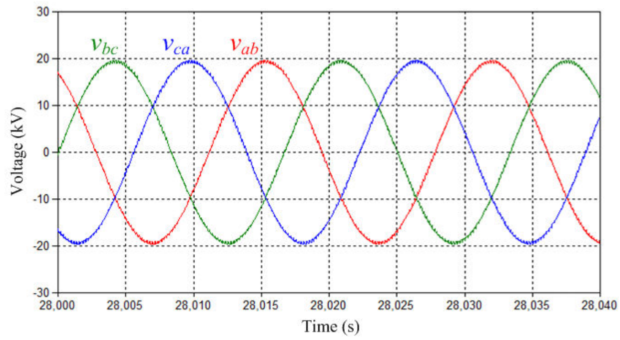


Fig. 6 Three-phase voltage zooms at the PCC with steady state 9m/s wind conditions – Case 1

The three line currents at the PCC, during the overall period of study, are illustrated at Fig 7. The waveforms make clear the oscillations caused by the wind speed characteristics (constant, gust and rump) and the control action at limiting the values. It is important to point out that the supplied electrical power delivered at the PCC is dependent on the cube of wind speed and on the power coefficients. This explains the variable values for the current amplitude along the studied time interval.

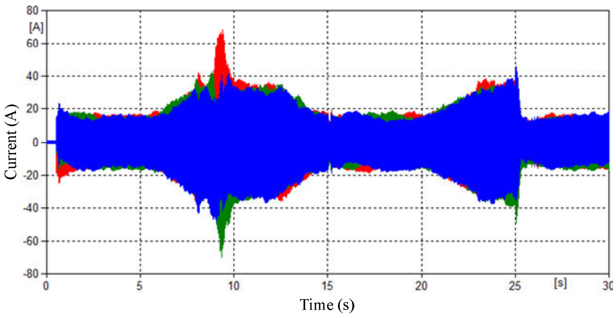


Fig. 7. Three phase line currents delivered by the wind farm to the PCC– Case 1

Figure 8 gives the active power produced by the wind farm and injected in the AC grid. It is clear that the injected power is in close agreement with the generator shaft power until the inverter control acts to optimize the $C_p$. The peak value of the active power is about 600 kW. If no Pitch control is considered then the value would be around 850 kW.

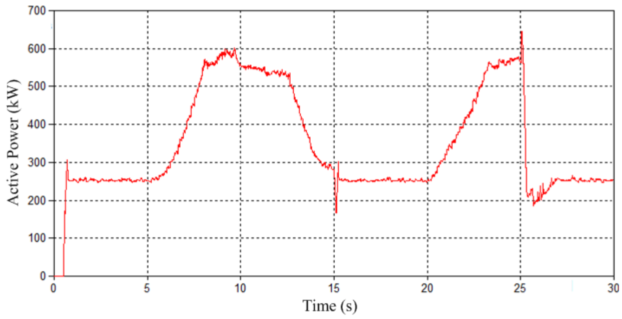


Fig. 8. Active power produced by the wind farm at the PCC – Case 1

The power control limitation via the reduction of energy transference to the wind turbine throughout the $C_p$ variable can be promptly observed in Fig. 9. This shows that at higher wind speed the Pitch control acts in such a way to reduce the value of $C_p$ so as to guarantee that no generator overload conditions will be allowed.

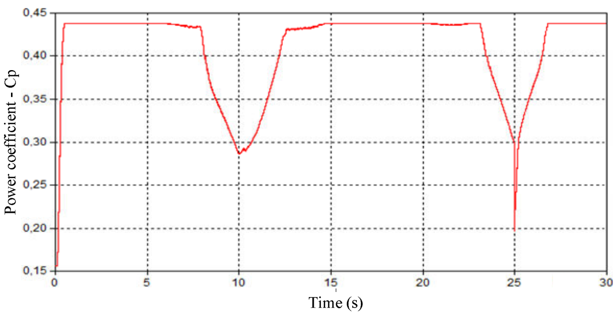


Fig. 9. Pitch control action and $C_p$ performance at limiting the energy transference to the wind turbine. - Case 1

## B. *Case 2 results*

This case is corresponding to the same wind conditions previously stated and other conditions expected by the PCC voltage which is now taken as having a established initial distortion related to 7% of 5th order voltage and 5% of 7th order component. This is associated to a voltage THD of about 9%.

Due to the fact that the imposed wind is the same previously defined no further information will be given to this energy source to the wind farm.

In a similar way to the above procedure at presenting results for Case 1, the following variables are given in the sequence:

- Line inverter output voltage ($v_{ab}$) zoom with steady state 9m/s wind conditions – Figure 10;
- Line voltages zooms at the PCC with steady state 9m/s wind conditions – Figure 11;
- Three-phase line currents produced by the wind farm at the PCC during the overall period of study – Figure 12;
- Active power produced by the wind farm over the studied time interval – Figure 13.

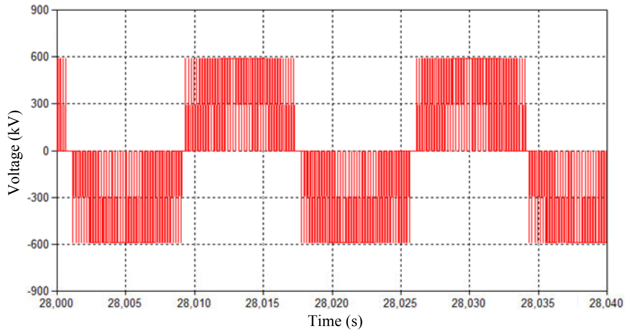


Fig. 10 Line voltage zoom waveform at inverter output with steady state 9m/s wind conditions – $v_{ab}$ - Case 2

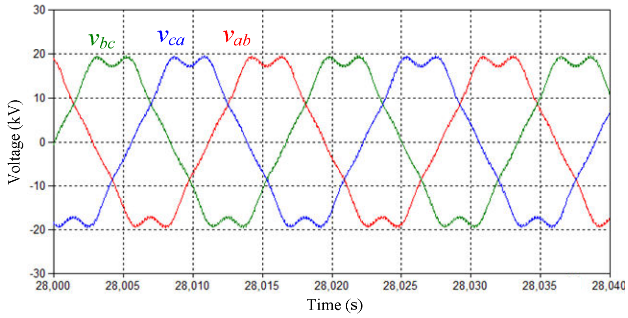


Fig. 11 Three-phase voltage zooms at the PCC with steady state 9m/s wind conditions – Case 2

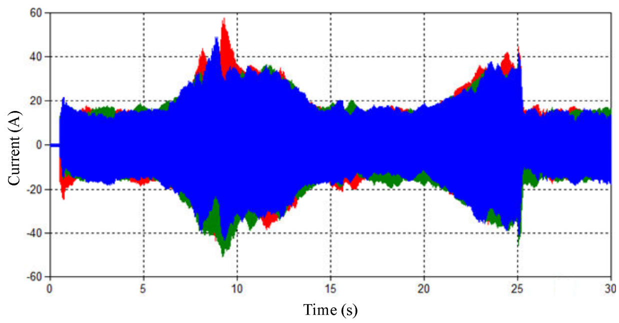


Fig.12. Three phase line currents delivered by the wind farm to the PCC– Case 2

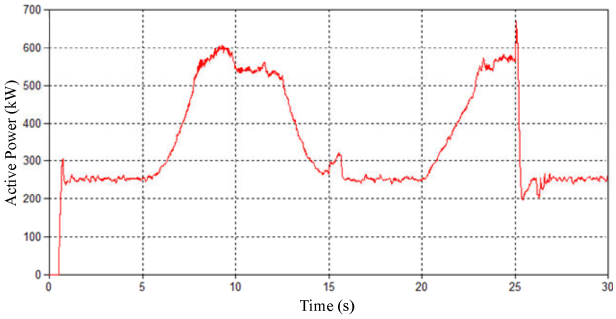


Fig. 13. Active power produced by the wind farm at the PCC – Case 2

Once again, the overall voltage profile has been omitted as it does not highlight any relevant information. The results here attached make clear that the distorted PCC voltage will not produce any appreciable effect on the wind farm complex operation conditions. The final voltage distortion was maintained around the same level previously adopted. This is in agreement with the fact that the generation unit here discussed does not have a major contribution to the THD. As far as the Cp is concerned to changes were found to justify the inclusion of a new figure.

### C. *Case 3 results*

With this new operating condition which has been assumed with 5% of voltage unbalance at the PCC, the studies were carried out and the following information have been selected for presentation and discussion:

- Line inverter output voltage ($v_{ab}$) zoom with steady state 9m/s wind conditions – Figure 14;
- Line voltages zooms at the PCC with steady state 9m/s wind conditions – Figure 15;
- Three-phase line currents produced by the wind farm at the PCC during the overall period of study – Figure 16;
- Active power produced by the wind farm over the studied time interval – Figure 17.

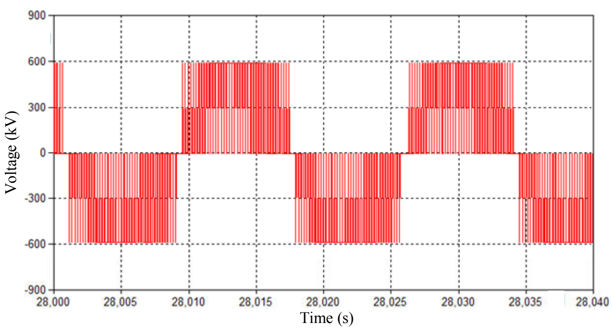


Fig. 14. Line voltage zoom waveform at inverter output with steady state 9m/s wind conditions – $v_{ab}$ - Case 3

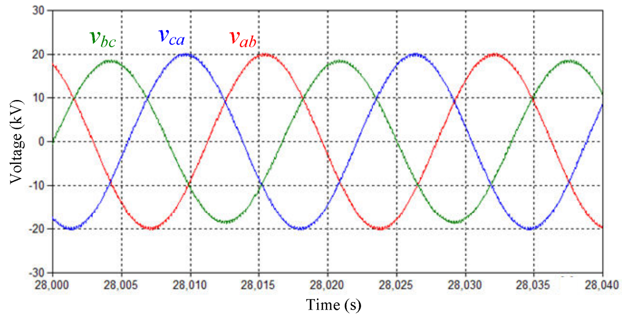


Fig. 15. Three-phase voltage zooms at the PCC with steady state 9m/s wind conditions – Case 3

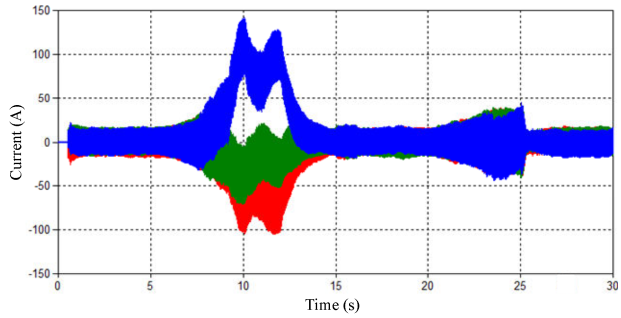


Fig. 16 Three phase line currents delivered by the wind farm to the PCC– Case 3

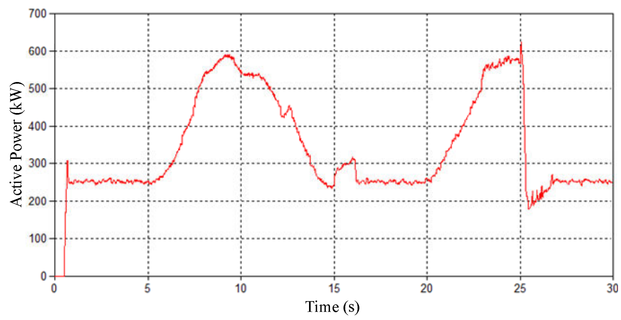


Fig. 17. Active power produced by the wind farm at the PCC – Case 3

The above waveforms are clear enough to demonstrate that the assumed level of PCC voltage unbalance will not produce any significant impact on the wind farm complex. No major influence was found to the performance variables. The initial unbalance level of 5% has not been affected and the THD have been slightly increased to about 1.5%.

## 4. Conclusion

This paper described the physical structure of a conventional type of variable speed Wind Energy Conversion System (WECS) and the time domain models for the individual components. The arrangement and corresponding equations were then implemented in the well known ATP platform so as to achieve a computational tool to deal with ideal and non-ideal operation conditions at both the WECS and the AC grid connection system. The three-phase independent representation for the wind farm and the AC busbar allows for considering abnormal operating conditions such as: AC busbar distortions, unbalances, voltage oscillations, etc.. Besides the general wind composition, any asymmetry associated to the wind farm electrical components is also available for a prompt use. Therefore, the computational package has the potentiality for power quality studies so as to evaluate WECS and PCC ideal and non-ideal operating conditions and their impact on the overall arrangement.

To illustrate the software application, three cases were selected to be discussed. They are involved with a more realistic wind composition where gust and ramp occurrences were added to a constant value. The idea was to focus typical wind profiles to emphasize the resulting voltage, current and power at the PCC. In a general way, it has been seen that with the imposed wind source, no further power quality problems related to THD, voltage unbalance and voltage oscillation were found at the PCC. In addition, the adoption of initial PCC voltage distortion and unbalance has not produced any appreciable effect on the overall system operations. This has highlighted that wind farm installations have a good withstand capability to overcome connection busbar non ideal conditions. Naturally, the authors cannot guarantee that this degree of immunity can be readily extended to other operating conditions.

The control units here considered, i.e. the Cp optimization and the Pitch facility have shown to be effective, respectively, at transferring the maximum power and at limiting the wind energy input at the generator shaft.

Finally, it must be emphasized that, due to the lack of published information related to WECS equipped with synchronous generators, the computational results have not yet been compared to real scheme performances. Despite that, a great effort is been made in order to assembly a WECS prototype so as to validate the simulation results here discussed.

## Acknowledgement

The authors acknowledge the financial support received from CNPq ,FAPEMIG, CAPES and Furnas Power Utility throughout its Power and Research Program.

## References

[1]S. Heier, "Grid Integration of Wind Energy Conversion Systems", John Wiley & Sons, England, 1998.

[2]J. G. Slootweg, H. Polinder, W. L. Kling, "Representing Wind Turbine Electrical Generating Systems in Fundamental Frequency Simulations", *IEEE Transactions on Energy Conversion*, Vol. 18, N°. 4, 2003, pp. 516 - 524.

[3]L. H. Hansen, P. H. Madsen, F. Blaabjerg, H. C. Christensen, U. Lindhard, K. Eskildsen, "Generators and Power Electronics Technology for Wind Turbines", *Industrial Electronics Society, IECON'01 - 27th Annual Conference of the IEEE*, Vol. 3, November, 2001, pp. 2000 - 2005.

[4]P. M. Anderson, A. Bose, "Stability Simulation of Wind Turbine Systems", *IEEE Transactions on Power Apparatus and Systems*, Vol. PAS 102, N° 12, 1983, pp. 3791 - 3795.

[5] Kundur, P. Power System Stability and Control. [S.l.]: McGraw-Hill, Inc, 1994.

[6]C. Schauder, H. Mehta, "*Vector Analysis and Control of Advanced Static Var Compensators*", *IEE Proceedings-C*, Vol. 40, N°. 4 Julho 1993, pp. 299 - 306.

[7]Kazmierkowski, M. P., Krishnan, R., Blaabjerg*, F. "Control Power Electronics - Selected Problems".* Orlando , USA, Elsevier Science, 2002. 518 p.

[8] Lee, D. C., Lee, G. M. *"A novel overmodulation technique for space vector PWM inverters*". IEEE Transactions on Power Electronics, vol. 13, Nov. 1998, pp. 1144-1151.